

# **COMS OPHTHALMIC APPLICATORS USING I-125 SEEDS**

## **INFORMATION**

### **INTRODUCTION**

Brachytherapy using I-125 and a variety of other isotopes in removable episcleral plaques is often used in the treatment of ophthalmic tumors (2, 6, 8, 16, 20, 21, 23). Plaque based brachytherapy permits higher tumor doses with greater sparing of non-involved tissues compared to x-ray teletherapy. Plaque therapy is more accessible, and less expensive, time consuming, and labor intensive than heavy charged particle teletherapy (4, 9, 10). A Phase III national study, the Collaborative Ocular Melanoma Study (COMS), is currently comparing the efficacy of plaque brachytherapy for moderately large tumors (3 to 8 mm height) versus enucleation.

Ophthalmic plaques fall into two general categories: (a) those that are supplied as ophthalmic applicators (2, 3, 5, 16, 23) with relatively long lived isotopes (Co-60 and Ru-106) and (b) those into which sealed radioisotope sources (Ir-192 or I-125) are temporarily inserted (1, 6, 12, 17, 21). The COMS participants use five standard sizes of sealed source plaques (6, 12). These plaques consist of a bowl shaped outer shell made of a gold alloy and a seed carrier insert made of silicone rubber. The silicone insert simplifies seed installation and offsets the seeds by 1 mm from the scleral surface. The gold shell is a symmetrical segment of a spherical surface which is terminated by a cylindrical lip of about 3 mm height. The lip holds the silicone insert and provides limited collimation of the photon flux from the plaque. Projecting from the lip are small eyelets which are used to suture the plaque to the sclera. Plaque diameters of 12 mm, 14 mm, 16 mm, 18 mm and 20 mm, measured at the lip, are available (Trachsel Dental Studio, Rochester, Minnesota, USA.). I-125 is the isotope designated (6) by the COMS. Sealed I-125 sources in the form of seeds are placed into the slots of the seed carrier, which is then inserted into the gold shell. The COMS plaques are pictured in Figure 1. Many alternatives to the COMS plaques have been reported in the literature for I-125 and Ir-192 seeds. Some of these alternatives permit asymmetrical designs (17, 21) and/or the incorporation of hyperthermia (1, 7). Asymmetrical plaques combined with a low energy isotope are particularly suited to treating tumors in close proximity to the optic nerve or macula.

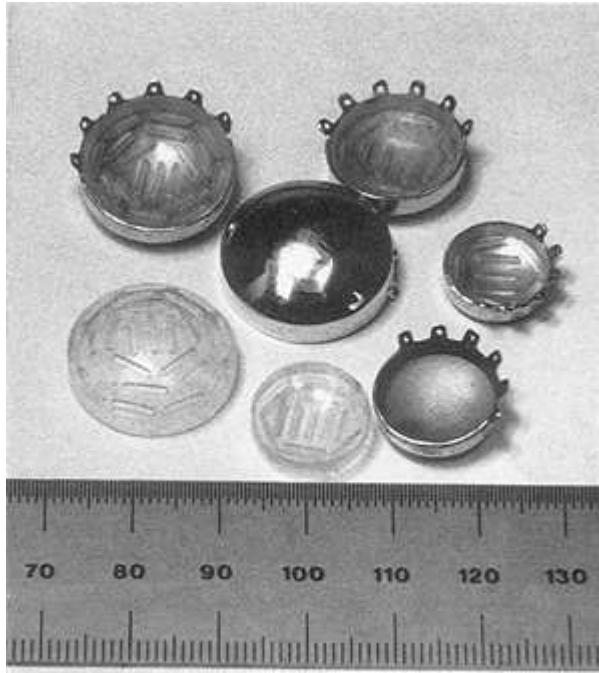


Fig. 1. The plaques used in the Collaborative Ocular Melanoma Study (COMS) have diameters ranging from 12 to 20 mm, and lip heights from 2.5 to 3.3 mm. I-125 seeds are loaded into a silicon carrier which is then inserted into the 0.5 mm thick gold alloy shell. The silicon carrier offsets the seeds by 1 mm from the scleral surface. Six suture eyelets project from the lip of a plaque at 30° intervals.

While initial tumor responses following ophthalmic radiotherapy have been good, late complications continue to be reported. Complications include scleral necrosis, macular edema, cataract, neovascular glaucoma and vasculopathy of the retina and optic nerve (5, 8, 11, 20, 22). It is of interest to obtain precise dosimetry in the immediate vicinity of ophthalmic plaques to determine if such data will correlate strongly with complications of treatment.

In this report we describe an ophthalmic plaque dosimetry program, implemented on a microcomputer workstation, which uses a highly interactive 3-dimensional graphics interface. The program provides detailed dosimetry for the COMS plaques, and has general application to all seed carrying plaques. In particular, isotope decay, source anisotropy, inhomogeneous scatter, and collimation provided by the lip at the edge of a plaque are accounted for.

## METHODS AND MATERIALS

### *Computer system*

The dosimetry program was originally developed on a personal computer (PC-XT, IBM Corporation, Boca Raton, FL, USA.), and subsequently adapted to the multiwindow environment of an inexpensive workstation (Macintosh II, Apple Computer Inc., Sunnyvale, CA, USA.) The original version was coded (Turbo Pascal 3.0, 8087 version, Borland International, Scotts Valley, CA, USA.) using a commercial graphics primitives (Halo™, Media Cybernetics, VA, USA.) library. The current version is coded (LightspeedC 3.0, Symantec, Bedford, MA, USA.) using the workstation's graphics "toolbox". The workstation displays 640 X 480 pixels at 72 ppi and 256 colors per pixel. The color graphics in this article were photographed from the workstation's video monitor.

## Plaque files

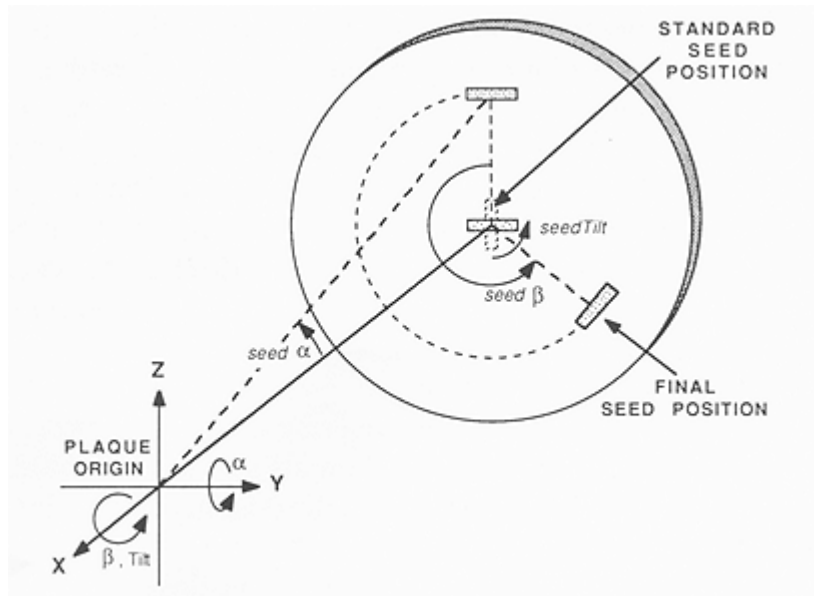


Fig. 2. The origin of a plaque's coordinate system is the center of the sphere to which it conforms. The position and orientation of a slot is specified by 3 angles which describe the displacement from a standard position and orientation. The seed is first rotated about the x-axis by seedTilt, then rotated about the y-axis by seed  $\alpha$ , and finally rotated about the x-axis once again by seed  $\beta$ .

Digitizing the coordinates of individual seeds for dosimetric purposes is laborious and prone to inaccuracy. This task can be simplified by observing that the seeds occupy fixed, standardized positions with respect to the silicon carrier and gold shell. If the location and orientation of the plaque is known, precise seed coordinates can be derived from a model of the plaque's structure. A plaque data file identifies the location, length, orientation and contents (I-125, Ir-192, or empty) of slots into which sealed sources can be loaded, and the radius of the sphere (plaqRadius in Fig. 3) to which the plaque conforms. The origin of the plaque's coordinate system is the center of this sphere. Three angles define the orientation and displacement of each source from a standard orientation and position. Referring to Figs 2 and 3, the standard position is defined as  $x = -(\text{plaqRadius} + \text{seedOffset})$ ,  $y = 0$ ,  $z = 0$ . The standard orientation has the long axis of the source parallel to the z-axis (seedTilt =  $0^\circ$ ). The seed is first rotated about the x-axis by seedTilt, then about the y-axis by seed  $\alpha$ , and finally rotated about the x-axis once again by seed  $\beta$ . A plaque description also includes the thickness of the plaque on the central axis (caxHeight), the location of suture eyelets, and a table of 24 radii which approximate the perimeter of the gold shell. The angular interval between radii is typically  $15^\circ$ , although they may be distributed irregularly if desired. A plaque file is created by measuring the plaque parameters and writing a computer program to create the plaque file algorithmically, by digitizing the plaque outline and slots from photographic frontal views, and/or by editing an existing plaque using interactive graphics.

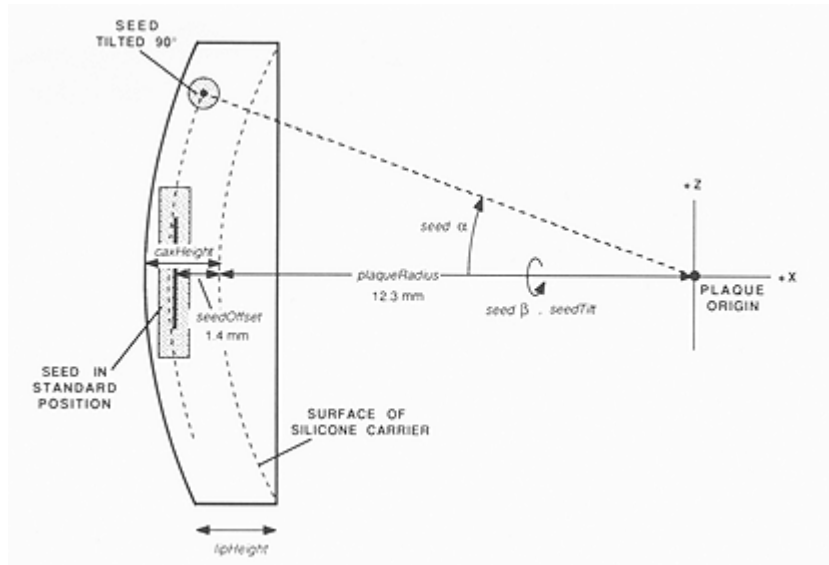


Fig. 3. Lateral view of the plaque coordinate system. A slot is initialized with its geometrical center at a standard position ( $x = -(\text{plaqRadius} + \text{seedOffset})$ ,  $y = 0$ ,  $z = 0$ ) and oriented with its long axis parallel to the  $z$ -axis ( $\text{seedTilt} = 0^\circ$ ).

A plaque description can be modified by changing the isotope loading pattern or the appearance of the plaque itself. A plaque editing window provides an expanded frontal view of the plaque in an interactive graphics mode. The mouse and screen pointer are used to install or remove seeds from a slot by pointing at the slot and "clicking" the mouse button. Standard default settings for isotope, source activity, implant duration, and other plaque related parameters are modified from "pull-down" menus and dialog windows, and may be overridden for individual seeds. Any combination of source activity and type is permitted. In addition, patterns of slots may be added or removed from the plaque and slot positions moved to new locations on the plaque using the interactive graphics interface. The plaque perimeter can be modified to indicate asymmetrical characteristics such as notches and suture eyelets. The modified plaque can be renamed and saved to disk for future use. The interactive editing capability permits custom plaque descriptions to be rapidly created from a library of previous patients and plaque designs.

*Positioning the plaque on the eye*

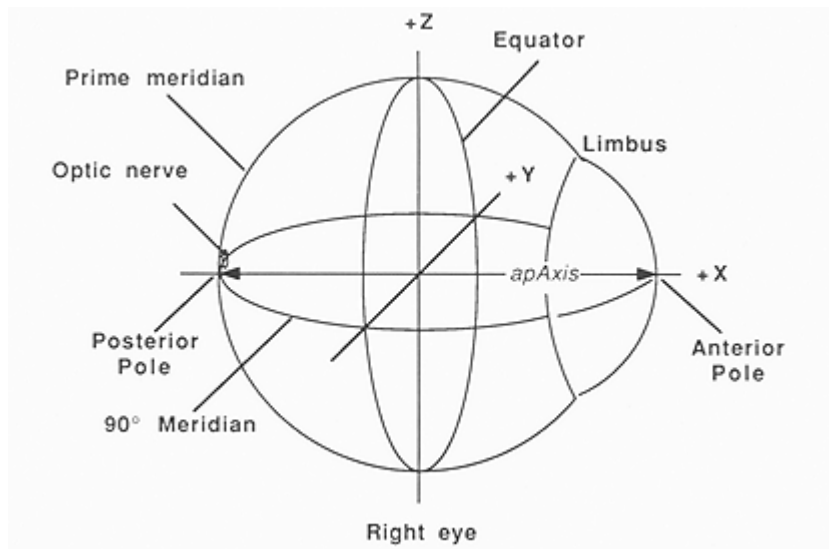


Fig. 4. The coordinate system used to indicate location on the surface of the eye. Latitude and longitude are specified with respect to the equator and prime meridian. The prime meridian begins at the posterior pole and passes through the positive z-axis. The positive y-axis is directed "away" from the viewer.

The position of the plaque during treatment is defined using a spherical, solid surface, 3D perspective projection of the eye. Left or right eye, anterior to posterior pole length (apAxis, Fig. 4), the diameter of the limbus and equator, and other ocular dimensions obtained from CT, MRI, ultrasound and/or direct caliper measurement are specified from menus and interactive dialogs. The eye, and markers for anatomical structures such as optic nerve are then dimensionally scaled to these parameters using the size and anatomic descriptions of Newell (19), Last (13), and the COMS. Displays for anterior, posterior, medial, lateral, superior or inferior views, as well as free rotation in three dimensions may be selected from a menu. To achieve the display speed necessary for smooth animation, the eye is drawn as a wire frame outline without hidden line removal during free rotation. Calculating and redrawing the solid-surface display requires about 2 seconds, which is too slow for animation. A "zoom" feature allows magnification of the screen image by up to 5 times to facilitate precise positioning of the plaque. The position of the geometrical center of a plaque during treatment is specified by "grabbing" the image of the plaque on the screen using the mouse controlled screen pointer, and "dragging" an animated, 3D wire frame outline of the plaque to the desired location. Alternatively, the plaque can be automatically centered over the tumor. The rotational orientation of the plaque with respect to its central axis is also specified interactively or from a dialog window.

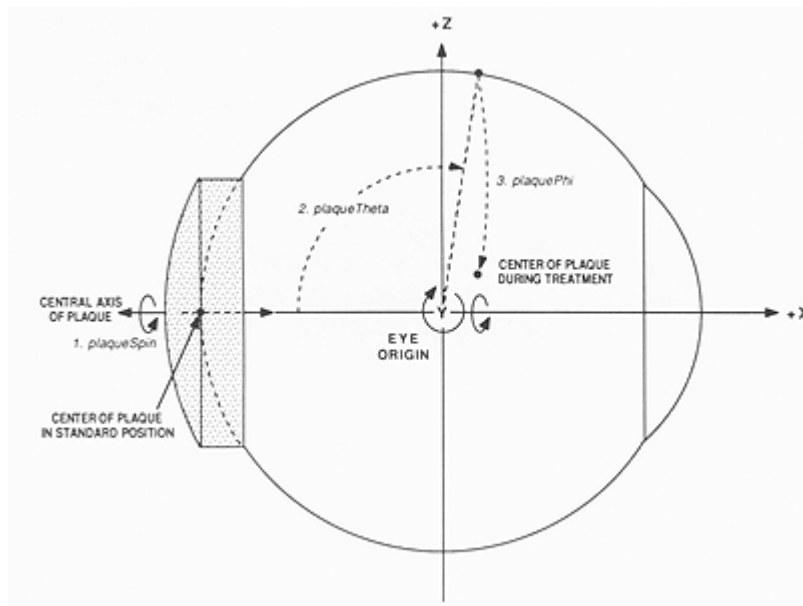


Fig. 5. Lateral view of the eye coordinate system. Although the operator of the program uses the more familiar terms of latitude and longitude to describe the plaque position, within the program the position and orientation of the plaque is handled as a sequence of angular displacements from the standard position in the local coordinate system of the eye. The plaque is first spun about its own central axis (plaqueSpin) to account for orientation, then rotated about the y-axis (plaqueTheta), and finally rotated about the x-axis once again (plaquePhi) to bring its center to the desired position.

Within the program, the position and orientation of the plaque are handled in a manner similar to that used to describe seed locations within a plaque. The plaque is initialized in a standard geometrical position and orientation with its center at the posterior pole of the eye. Figure 4 illustrates the location of the poles, equator, limbus, and meridians with respect to the anatomy of the eye. The latitude and longitude of the plaque center, and the orientation of the plaque during treatment are converted into a sequence of rotations from the standard position (in the local coordinate system of the eye). Referring to Figure 5, the plaque is first spun about its own central axis (plaqueSpin) to account for orientation. In the standard geometry, the central axis of the plaque is the same as the x-axis of the eye, so this involves a rotation about the x-axis. The plaque is then rotated about the y-axis (plaqueTheta), and finally rotated about the x-axis once again (plaquePhi) to bring its center to the desired position.

### *Calculating and displaying the dose distribution*

Transverse, sagittal, or coronal planar cross-sections may be requested, as well as any plane transecting the eye diametrically. These planar surfaces are displayed within a translucent eye. In addition, any spherical surface within or surrounding the eye can be displayed as a 3-dimensional perspective projection or as a funduscopy (or "retinal") diagram. Interactive zoom and pan on the dosimetry surface is provided. Dose calculation matrices ranging from 20 X 20 to 160 X 160 points may be selected. The matrix may be applied to a planar dosimetry surface in any rectangular subregion ranging from 2 to 40 mm on edge. Bilinear interpolation is used to estimate isodose contours between the calculated points. A variety of color and grey scale isodose display options are provided including a library of predefined formats covering one to four orders of magnitude. User definable formats are also available. The display can

be normalized to the dose at any location on the central axis of the plaque or the apex of the tumor. Alternatively, the dose at any point on the dosimetry surface can be calculated explicitly and displayed numerically by "clicking" the pointer at the location. A table of dose values at 1 mm intervals on the central axis of the plaque, and to the center of certain ocular structures is also available.

The dosimetry algorithm initially treats each seed as an unfiltered line source, located on the longitudinal axis of the physical seed, in a full scatter geometry. Various dose modifying factors, taken from the literature and from our own measurements are then applied to account for tissue attenuation and scatter (15), angular anisotropy (14, 25), and deviation from full scatter geometry due to the gold shell (18). The activity of each source at the start of treatment is specified in the plaque description. Although the program defaults to a 1 hr calculation, any calculation period may be specified. Source decay is automatically included in the calculation. For sources which are offset from the scleral surface, the intervening medium is presumed to be tissue equivalent. The dose calculation model has been described previously, and compared to TLD measurements in an acrylic phantom (17).

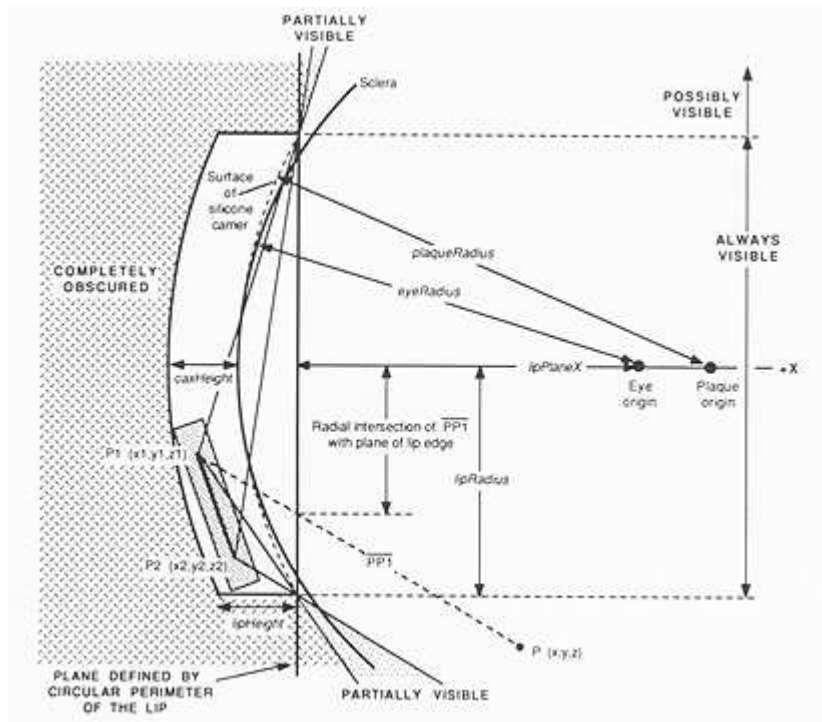


Fig. 6. Diagram of the standard geometry for plaques with a circular lip. This standard geometry simplifies the calculation of what portion of a seed is visible from an arbitrary position P in 3-dimensional space. See text for explanation.

Collimation of the direct photon fluence from each source by the lip of a plaque with a circular perimeter (any of the COMS plaques) is accounted for by considering the plaque to be in the standard geometry discussed above. Instead of rotating the plaque and its sources, the calculation point is rotated by the inverse transformation, bringing it to a corresponding location in the standard geometry. In the standard coordinate system, if the x coordinate of the rotated dosimetry point P (x, y, z) falls "behind" the plane defined by the circular perimeter of the plaque ( $x \leq -\text{lipPlaneX}$  in Fig. 6) then the position of P is compared to the structure of the gold shell. If P lies outside the cylinder defined by the lip (i.e.,  $(y^2 + z^2) > \text{lipRadius}^2$ ) or if P lies within the cylinder and behind the plaque (i.e.,  $(x < 0)$  and  $((x + \text{eyeRadius} - \text{plaqRadius})^2 + y^2 + z^2) >$

( $\text{plaqRadius} + \text{caxHeight}$ )<sup>2</sup>)) then the sources are completely obscured by the gold shell and the dose is modified by the transmission factor (for the particular isotope) through the gold. For I-125, the transmission is considered to be zero.

If the x coordinate of P lies in front of the plaque ( $x > -\text{lipPlaneX}$ ) and P lies within the cylinder defined by the lip, then the sources are always in direct sight, and the gold shell has no direct effect. If P lies outside the cylinder, then the intersections of lines between P and the endpoints of the seed (PPI and PP2) with the plane  $x = -\text{lipPlaneX}$  are calculated. Lines which intersect this plane within the circular perimeter of the lip indicate that the endpoint is visible from P, whereas lines which intersect outside the circle indicate an endpoint which is obscured by the lip. If both end points of a source are visible there is no lip attenuation. If both endpoints are obscured, the gold transmission factor is applied. If one endpoint is visible and the other is obscured, the source is partially visible and an iterative procedure is used to estimate the "partial visibility ratio" ( $\text{pvr} = \text{visible length} / \text{source length}$ ). The gold transmission factor is applied only to the portion of the seed which is obscured. An iterative algorithm was chosen to estimate the pvr in order to reduce computational complexity. The dosimetry algorithms are available from the author.

The lip calculation currently considers only the primary photon flux from a source. Luxton et al (17) have observed that backscatter from an eye phantom shielded by a plaque is about 3% of the unshielded exposure rate. This suggests that scatter into shielded regions away from the penumbral region is not of great clinical significance. The relative contribution of scatter to the penumbral region, however, is unknown. At this time we must consider that our calculation underestimates dose in the penumbral region.



# An Interactive Treatment Planning System For Ophthalmic Plaque Radiotherapy

Melvin A. Astrahan, PH.D.,<sup>1</sup> Gary Luxton, PH.D.,<sup>1</sup> Gabor Jozsef, PH.D.,<sup>1</sup> Thomas D. Kampp, PH.D.,<sup>1</sup> Peter E. Liggett, M.D.,<sup>2</sup> Michael D. Sapozink M.D., PH.D.<sup>1</sup> AND Zbigniew Petrovich, M.D.<sup>1</sup>

*Int. J. Radiation Oncology, Biol, Phys., Vol. 18, pp. 679-687 Copyright 1990 Pergamon Press*

1. Department of Radiation Oncology.
2. Department of Ophthalmology.

University of Southern California School of Medicine, Los Angeles, California, USA

---

## ABSTRACT

Brachytherapy using removable episcleral plaques containing sealed radioisotope sources is being studied as an alternative to enucleation in the treatment of choroidal melanoma and other tumors of the eye. Encouraging early results have been reported, but late complications which lead to loss of vision continue to be a problem. A randomized national study, the Collaborative Ocular Melanoma Study (COMS) is currently in progress to evaluate the procedure. The COMS specified isotope is I-125. Precise dosimetric calculations near the plaque may correlate strongly with complications and could also be used to optimize isotope loading patterns in the plaques. A microcomputer based treatment planning system has been developed for ophthalmic plaque brachytherapy. The program incorporates an interactive, 3-dimensional, solid-surface, color-graphic interface. The program currently supports I-125 and Ir-192 seeds which are treated as anisotropic line sources. Collimation effects related to plaque structure are accounted for, permitting detailed study of shielding effectiveness near the lip of a plaque. A dose distribution matrix may be calculated in any subregion of a transverse, sagittal, or coronal planar cross section of the eye, in any plane transecting the plaque and crossing the eye diametrically, or on a spherical surface within or surrounding the eye. Spherical surfaces may be displayed as 3-dimensional perspective projections or as funduscopy diagrams. Isodose contours are interpolated from the dose matrix. A pointer is also available to explicitly calculate and display dose at any location on the dosimetry surface. An interactive editing capability allows new plaque designs to be rapidly added to the system.

Key words: I-125, Plaque, Choroidal melanoma, Radiation dosimetry.

Accepted for publication 19 July 1989.

## DISCUSSION

This program can potentially be applied to optimize plaque design, seed placement, and treatment planning. For example, in the geometry depicted in Figure 10, if the dose at the 6 mm normalization point were 100 Gy, then the estimated dose to the center of the optic disc would be about 80 Gy without accounting for lip collimation, and about half that when lip collimation is included. If a 40 Gy variation in dose to a critical structure were associated with a significant difference in complication rate, the ability to account for lip collimation will be important. In addition to plaque orientation, the effects of using mixed isotopes, and/or seeds of unequal activity can be modelled. This may be of value in reusing sources and tailoring the dose distribution to an irregular tumor volume. The ability to immediately display point dose values without necessarily calculating a complete dose matrix provides rapid feedback for plaque design, and permits detailed study of dose gradients within structures such as the lens, optic disc or macula.

Absolute dosimetry for plaques containing Ir-192 seeds, and relative dosimetry for I-125 seeds, were compared to TLD measurements in an acrylic phantom for the calculational model used in this program by Luxton et al. (17). The dosimetry for I-125 seeds, however, should be considered only approximate at this time. Recent Monte Carlo evaluations by Williamson (24) suggest that characteristic X rays from the titanium seed capsule may lead to a 7% overestimate of the specific dose constant when calibration is performed in air. These low energy photons are rapidly absorbed in water-like media and therefore have negligible contribution to tissue dose at distances greater than 0.5 mm. Williamson (24) suggests a specific dose constant (the ratio of absolute dose rate at 1 cm on the transverse bisector of a seed in a specific medium to the source strength) of 0.909 for the model 6711 seed. This is about 14% lower than the 1.035 value recommended by Ling et al. (15) for the same model seed. In light of the present uncertainties concerning the absolute dosimetry of I-125 seeds, all dose distributions reported here were normalized to a point on the central axis of the plaque, 6.0 mm from the plaque surface, and near the apex of a hypothetical 5 mm tumor. This represents a typical dose specification point at this institution and by the COMS.

The multi-window, 3-dimensional graphics interface provides an intuitive environment for both the physicist and physician to work within. Goitein and Miller (9) used a similar approach for planning proton therapy of the eye. This earlier work was implemented in FORTRAN on a computer (VAX 11/780) and required about 1.3 full-time-equivalent (FTE) man-years to implement. The program described here was developed in about 0.4 FTE man-years with the aid of the ROM "toolbox" functions built into the Macintosh computer. Since the program adheres to the recommended user interface guidelines, it is simple to learn and use, and is an example of how this new hardware and software technology can be rapidly and successfully applied to clinical dosimetry tasks.

There are several aspects of the current dosimetry system which require refinement prior to clinical implementation. The generalized approximation of intraocular anatomy within a spherical globe may be too imprecise for many variants of human ocular anatomy. Digitization of the tumor perimeter from fundus photography, estimation of the 3-dimensional tumor volume from sequential CT or MRI images,

and display of the 3-dimensional tumor volume within a translucent eye would be desirable additions. These would provide visual aids during plaque positioning and permit correlation of isodose surfaces with actual tumor and normal tissue contours. Surgical reproduction of the preplanned plaque orientation and location could be difficult to achieve. If the source locations are fixed relative to the suture eyelets on the plaque, however, and the spatial location of the suture eyelets relative to real anatomical landmarks, such as the limbus, can be specified, precise surgical placement may be facilitated. Three-dimensional isodose surface displays and loading optimization based on available isotope resources would also be desirable. The lip collimation algorithm currently assumes a circular lip. This could be refined to handle lips of arbitrarily shaped perimeters. The COMS plaques use a silicone rubber carrier to offset the sources by 1 mm from the sclera. Our model presently considers this intervening medium to be tissue equivalent. For the low energy photons from I-125 seeds, photoelectric attenuation and scatter characteristics in silicone rubber could vary significantly from tissue and probably need to be accounted for. Dose resulting from scatter into the penumbral region close to the plaque perimeter is not modelled and may be of significance as well. We are presently adding these capabilities to the dosimetry system reported here.

## REFERENCES

1. Astrahan, M. A.; Liggett, P.; Petrovich, Z.; Luxton, G. A 500 KHz localized current field hyperthermia system for use with ophthalmic plaque radiotherapy. *Int. J. Hyperther.* 3:423-432; 1987.
2. Brady, L. S.; Shields, J. A.; Augsburger, J. J.; Day, J. L. Malignant intraocular tumors. *Cancer* 49:578-585; 1982.
3. Chan, B.; Rotman, M.; Randall, G. J. Computerized dosimetry of <sup>60</sup>Co ophthalmic applicators. *Radiology* 103:705-707; 1972.
4. Char, D. H.; Castro, J. R.; Stone, R. D.; Irvine, A. R.; Barricks, M.; Crawford, J. B.; Schatz, H. A.; Lonn, L. L.; Hilton, G. F.; Schwartz, A.; Quivey, J. M.; Saunders, W.; Chen, G. T. Y.; Lyman, J. T. Helium ion therapy for choroidal melanoma. *Arch. Ophthalmol.* 100:935-938; 1982.
5. Char, D. H.; Lonn, L. L.; Margolis, L. W. Complications of cobalt plaque therapy of choroidal melanomas. *Am. J. Ophthalmol.* 84:536-541; 1977.
6. Earle, J.; Kline, R. W.; Robertson, D. M. Selection of Iodine 125 for the Collaborative Ocular Melanoma Study. *Arch. Ophthalmol.* 105:763-764; 1987.
7. Finger, P. T.; Packer, S.; Svitra, P. P.; Paglione, R. W.; Anderson, L. L.; Kim, J. H.; Jakobiec, F. A. Thermoradiotherapy for intraocular tumors. *Arch. Ophthalmol.* 103: 1574-1578; 1985.
8. Garretson, B. R.; Robertson, D. M.; Earle, J. D. Choroidal Melanoma treatment with Iodine 125 brachytherapy. *Arch. Ophthalmol.* 105:1394-1397; 1987.
9. Goitein, M.; Miller, T. Planning proton therapy of the eye. *Med. Phys.* 10:275-283; 1983.
10. Gragoudas, E. S.; Goitein, M.; Verhey, L.; Munzenreider, J. E.; Urie, M.; Suit, H. D.; Koehler, A. Proton beam irradiation of uveal melanomas; results of a 5' year study. *Arch. Ophthalmol.* 100:928-934; 1982.

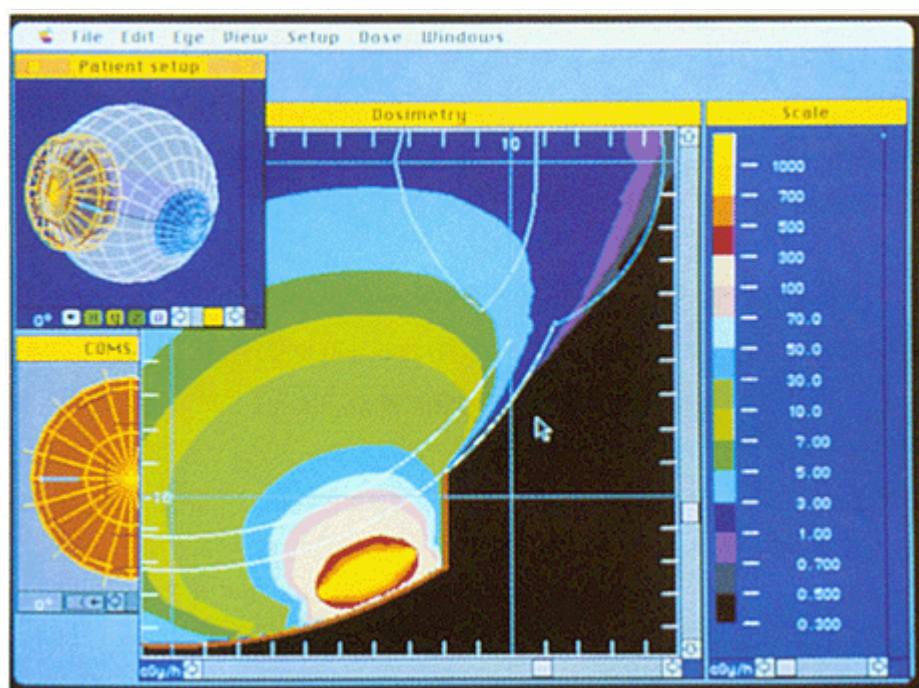
11. Haik, B. G.; Jereb, E. B.; Abramson, D. H.; Ellsworth, R. M. Ophthalmic radiotherapy. In: Iliff, N., ed. Complications in ophthalmic therapy. New York: Churchill Livingstone; 1983:449-485.
12. Kline, R. W.; Yeakel, P. D. Ocular melanoma, I-125 plaques. Med. Phys. 14:475; 1987 (abstract).
13. Last, R. J. (Wolff's) Anatomy of the eye and orbit, 6th edition. Philadelphia and Toronto: W. B. Saunders Company; 1968:30.
14. Ling, C. C.; Schell, M. C.; Yorke, E. D. Two-dimensional dose distribution of I-125 seeds. Med. Phys. 12:652-655; 1985.
15. Ling, C. C.; Yorke, E. D.; Spiro, I. J.; Kubiawicz, D.; Bennett, D. Physical dosimetry of I-125 seeds of a new design for interstitial implant. Int. J. Radiat. Oncol. Biol. Phys. 9: 1747-1752; 1983.
16. Lommatzsch, P. K.  $\beta$ -irradiation of choroidal melanoma with Ru-106/Rh-106 applicators. Arch. Ophthalmol. 101:713-717; 1983.
17. Luxton, G.; Astrahan, M. A.; Liggett, P.; Neblett, D. L.; Cohen, D. M.; Petrovich, Z. Dosimetric calculations and measurements of gold plaque ophthalmic irradiators using Iridium-192 and Iodine-125 seeds. Intl. J. Radiat. Oncol. Biol. Phys. 15:167-176; 1988.
18. Luxton, G.; Astrahan, M. A.; Petrovich, Z. Backscatter measurements from a single seed of 1211 for ophthalmic plaque dosimetry. Med. Phys. 15:397-400; 1988.
19. Newell, F. W. Ophthalmology principles and concepts, 4th edition. Saint Louis: C. V. Mosby Company; 1978:3-7.
20. Packer, S. Iodine-125 radiation of posterior uveal melanoma. Ophthalmology 94:1621-1626; 1987.
21. Packer, S.; Rotman, M. Radiotherapy of choroidal melanoma with Iodine-125. Ophthalmology 87:528-590; 1980.
22. Seddon, J. M.; Gragoudas, E. S.; Egan, K. M.; Glynn, R. J.; Munzenrider, J. E.; Austin-Seymour, M.; Goitein, M.; Verhey, L.; Urie, M.; Koehler, A. Uveal melanomas near the optic disc or fovea-visual results after proton beam irradiation. Ophthalmology 94:354-361; 1987.
23. Stallard, H. B. Radiotherapy for malignant melanoma of the choroid. Brit. J. Ophthalmol. 50:147-155; 1966.
24. Williamson, J. F. Monte Carlo evaluation of specific dose constants in water for I-125 seeds. Med. Phys. 15:686-694; 1988.
25. Williamson, J. F.; Morin, R. L.; Khan, F. M. Monte Carlo evaluation of the Sievert integral for brachytherapy dosimetry. Phys. Med. Biol. 28:1021-1032; 1983.

Acknowledgements - Portions of the original computer system used to help develop this program were provided through an education, research and development grant from IBM Corporation (University of Southern California project Socrates), and an American Cancer Society Institutional Research Grant ACS-IRG IN-21-W through the USC Comprehensive Cancer Center. The Macintosh II implementation was assisted in part by a gift from BSD Medical Corporation.

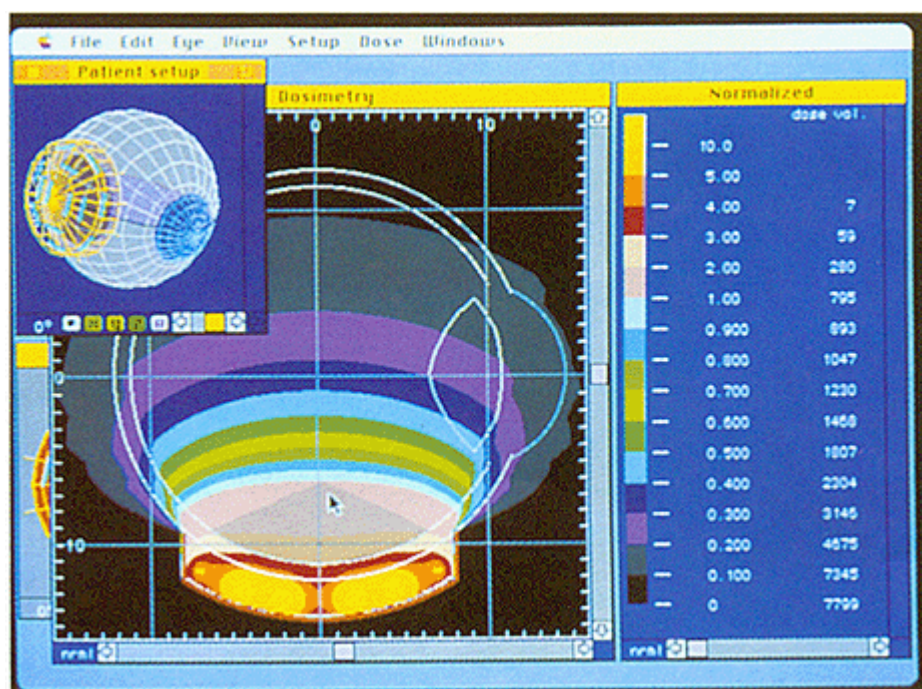
## RESULTS

The Macintosh implementation (16MHz 68020 processor) requires approximately 3 secs per seed to calculate a 40 X 40 dose matrix with lip detection activated, and is about 20% faster when lip detection is disabled. Interpolating the dose matrix and generating the screen display requires from 3 to 30 secs, depending only on the size of the display window and the type of display surface requested (planar or 3D perspective projection). The time required to generate a screen display is independent of the dose matrix resolution. Although matrices up to 160 X 160 points are available at the cost of proportionately longer computation time, no visual improvement in isodoses within the hypothetical tumor volume was apparent between the 40 X 40 and 80 X 80 modes. The higher resolution modes which generated the figures in this report are primarily intended to reduce aliasing in the penumbral region near the lip. A typical plaque with 10 seeds normally requires < 60 sec to calculate and display a dosimetry matrix adequate for clinical purposes, and about 1 sec to generate a dose table for the central axis and critical structures.

Fig. 7. Test of the partial visibility algorithm using a single I-125 source: (a) in a slot near the center of the plaque, (b) in a slot near the lip, (c) in a modified version of the plaque with a radially oriented slot near the lip. The plane of dose calculation is the plane  $z = 0$ .



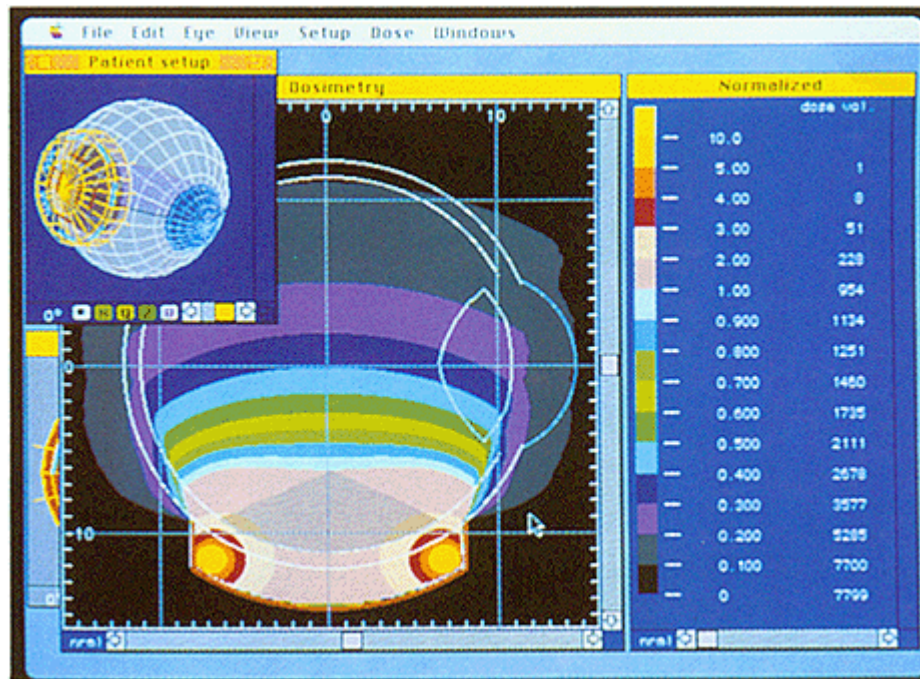
The partial visibility algorithm was tested using a 16 mm diameter COMS plaque. A single 4 mCi seed of I-125 was assigned to a slot near the center of the plaque (Fig. 7a), near the lip (Fig. 7b), and to a radially oriented slot near the lip of a modified plaque (Fig. 7c). The displayed isodose distributions are consistent with the expected shielding effects. Shielding of the sclera adjacent to the plaque is greatest for the seed near the lip and nonexistent for the centrally located seed. Some aliasing in the penumbral region is evident for the radially oriented seed, but is of little practical concern. This aliasing results from the limit of five iterations imposed (to improve speed) on the pvr calculation.



(a)

Fig. 8. Comparison of a peripheral loading pattern versus a uniform loading pattern for the COMS 16 mm diameter plaque. The dose distribution is calculated for the plane  $z = 0$ . The display has been normalized to a value of 1.0 at 6 mm from the plaque surface on the central axis of the plaque, near the apex of a hypothetical tumor. The nominal position of the retina is indicated by the inner white semi-circle, inset 1 mm from the scleral surface. The tumor is roughly conical in shape, and is indicated by the darkened region within the eye. Dose volume is calculated in  $\text{mm}^3$ . (a) 13 equal sources filling all available slots. (b) 7 equal sources in the peripheral ring.





(b)

Alternative loading patterns for the plaque were studied to model pre-treatment planning capability, again using the 16 mm COMS plaque loaded with I-125 seeds. The plaque was centered on the y-axis at the intersection of the equator and lateral (90°) meridian (Fig. 4). Dose matrices were calculated in the plane  $z = 0$  which transects both the plaque and eye. In the first case, 13 sources of equal activity filled all of the available slots in the plaque (Fig. 8a). This was compared to seven sources of equal activity in the peripheral ring of slots (Fig. 8b). The dose distributions of Figure 8 have been normalized to a value of 1.0 at 6 mm above the surface of the plaque near the apex of a hypothetical 5 mm tumor. While dose to the tumor volume appears to be similar, retinal dose appears to be more homogenous for the peripheral loading pattern. A dose-volume histogram for 1 mm<sup>3</sup> voxels within the eye was calculated for each case. The results indicate that the peripheral loading pattern increased the volume of eye tissue receiving a dose  $\geq 4X$  the normalization dose by only 1 mm<sup>3</sup> while decreasing the volume  $\geq 2X$  by 52 mm<sup>3</sup>. For this particular geometry, the improved homogeneity of the peripheral loading pattern was achieved at the cost of a slight increase in dose to the lens and to the sclera near the peripheral edge of the plaque.

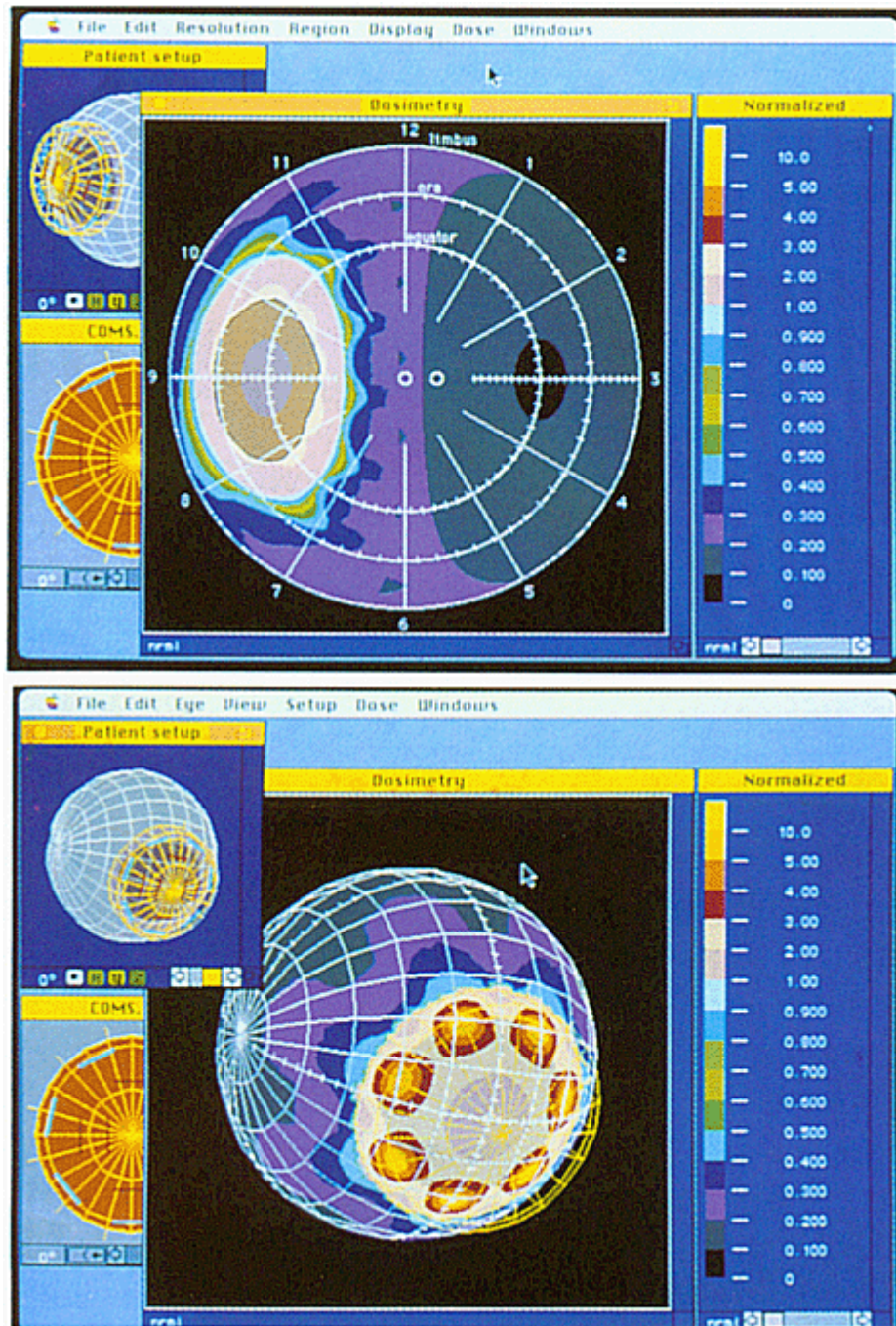


Fig. 9. Dose distributions on the scleral and retinal surfaces for the COMS 16 mm plaque with 7 equal I-125 sources in the peripheral ring. The display has been normalized to a value of 1.0 at 6 mm from the plaque surface on the central axis of the plaque. (a) 3-dimensional perspective projection view of the scleral dose distribution. (b) Funduscopy diagram of dose to the retina.

(a)

(b)

The dose distribution on the scleral surface and the retina (assumed to be 1 mm inset from the scleral surface) are modeled in Figures 9 & 10 for the plaque depicted in Figure 8b. All dosimetry is normalized as in Figure 8. The scleral dose distribution is plotted as a 3D perspective projection in Figure 9a. The retinal dose distribution is plotted in the manner of a funduscopy diagram in 9b. Localized areas of high dose on the sclera adjacent to each seed, which were not readily apparent in Fig. 8b are now clearly seen in Fig. 9a. Outside the lip perimeter indicated by the yellow wire-frame in



Figure 9a, a distinctive lobular pattern is observed in the 0.1 to 0.7 relative dose range. This pattern apparently results from partial visibility of alternating sources. Figures 10a & 10b display views of the retinal dose from anterior and posterior vantage points. Figure 10c is identical to 10b except that lip collimation is ignored. The dose distribution in Figure 10c suggests that the lip, rather than anisotropy is the source of the lobular pattern. For this particular geometry and orientation, in which the plaque is adjacent to the optic nerve, the calculated dose to the center of the optic disc in Figure 10c is roughly twice that of 10b.

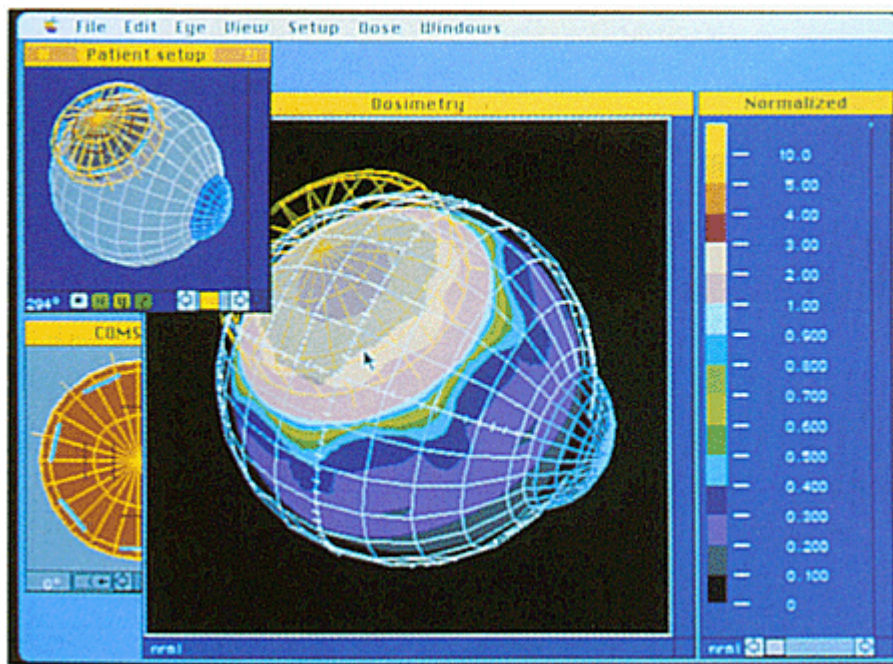
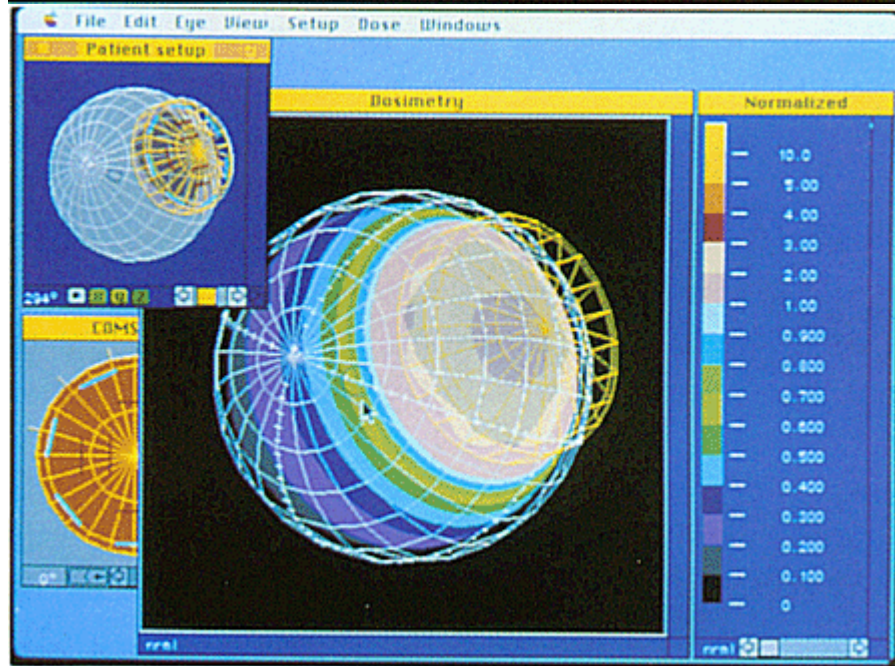
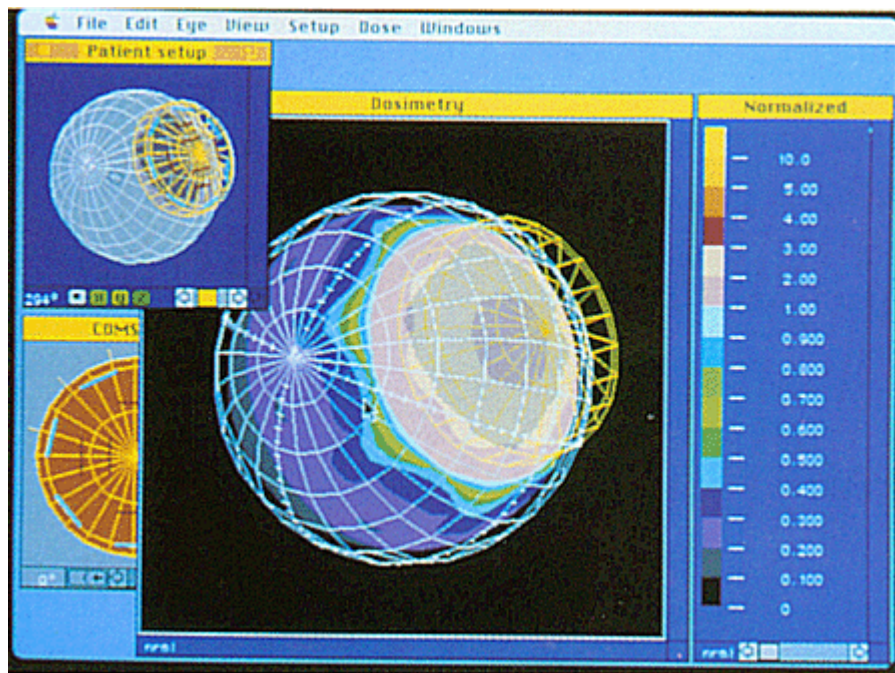


Fig. 10. Retinal dose distributions for the COMS 16 mra plaque with 7 equal I-125 sources in the peripheral ring. The display has been normalized to a value of 1.0 at 6 mm from the plaque surface on the central axis of the plaque. (a) and (b) are 3dimensional perspective projection views from anterior and posterior vantage points. (c) is identical to (b) except that lip collimation effects have been ignored.



(a)

(b)

(c)